Functional Analysis of Combinatorial Mutants with Changes in the C-Terminus of the CD Loop of the D2 Protein in Photosystem II of *Synechocystis* sp. PCC 6803†

Anna T. Keilty, Dmitrii V. Vavilin, and Wim F. J. Vermaas*

Department of Plant Biology and Center for the Study of Early Events in Photosynthesis, Arizona State University, Box 871601, Tempe, Arizona 85287-1601

Received December 6, 2000; Revised Manuscript Received January 24, 2001

ABSTRACT: Photosystem II properties were investigated in a set of combinatorial mutants containing changes in the C-terminal end of the CD lumenal loop (Gly187−Asn194) in the D2 protein of *Synechocystis* sp. PCC 6803. Initial screening of variable fluorescence (F_v) induction and decay in the presence of DCMU showed that all but one of the combinatorial strains tested had an increased rate of Q_A^- reoxidation. Two strains showed an increase in the amplitude of constant fluorescence (F_o). Examination of the primary sequence of the combinatorial strains combined with results obtained from analysis of site-directed mutants suggested that alterations in residue 191 of D2 increased the rate of charge recombination. Indeed, reintroduction of Trp191, the residue present in wild type, slowed the Q_A^- reoxidation rate in the presence of DCMU by 2−3-fold. However, the nature of other residues, in particular at codon 192, was also important in determining charge recombination rates. The increase in F_o yield was due to an increased fluorescence lifetime of open reaction centers in intact cells and may reflect a decreased excitation trapping rate in the reaction center. This change was reversed by reintroduction of Trp191 even though a mutant lacking just Trp191 was normal in this respect. Trapping efficiency therefore was decreased only when multiple changes were present at the same time. We interpret Trp191 and neighboring residues to influence the midpoint redox potential of P680/$P680^+$ and in certain sequence contexts to affect the energy trapping efficiency by P680. The stability or environment of Y_D^{ox} was essentially unaffected in the mutants. Interestingly, many combinatorial mutants displayed an increased requirement for chloride for photoautotrophic growth, and two mutants, C8-10 and C8-23, also required more calcium. This indicates that this CD loop region of D2 not only affects properties of P680 but also affects properties of the oxygen-evolving complex.

In photosystem II (PS II),[1] the oxidized primary donor, $P680^+$, is reduced by an electron from the redox-active tyrosine residue, Y_Z, which in turn is reduced by the oxygen-evolving complex (OEC) on the lumenal side of the thylakoid membrane. Y_Z (Tyr161 of D1 in *Synechocystis* sp. PCC 6803) (*1*, *2*) and a second redox-active tyrosine, Y_D (Tyr160 of D2) (*3*, *4*), which is not in the main pathway of electron flow, are located symmetrically at the base of the C helices of the D1 and D2 proteins, respectively, but they differ radically in their redox kinetics. Y_D oxidation occurs in the domain of seconds, and Y_D^{ox} is stable for hours or days. Y_Z is oxidized by $P680^+$ in nanoseconds, and Y_Z^{ox} is reduced by the OEC in micro- to milliseconds (reviewed in ref *5*). In both cases the oxidized Tyr transfers its proton to a nearby residue, resulting in a neutral radical. The most prominent proton-accepting residues are His190 of D1 for Y_Z and His189 of D2 for Y_D (*6*−*10*).

The functional role of Y_D is still a mystery. Y_D is dispensable, and the Y160F (D2) mutant is still photoautotrophic albeit somewhat impaired (*3*, *4*). A postulated function for this residue includes a role in photoactivation of PS II (*11*) possibly by serving as an auxiliary electron donor to $P680^+$ and/or Y_Z^{ox} to prevent photoinhibition during the photoactivation process (*12*, *13*).

The reasons for the functional differences between Y_Z and Y_D are still unclear but may be related to structural differences in regions of the D1 and D2 proteins, such as regions of the CD lumenal loop that surround the redox-active tyrosine residues. The CD lumenal loop region connects helix C and helix D of D1 and D2 at the lumenal side of the thylakoid membrane. On the basis of similarity with the purple bacterial reaction center the CD loop is believed to contain an α-helical region that interacts with the lumenal edge of the thylakoid membrane (*14*, *15*). While the CD loop may be structurally similar in the D1 and D2 proteins, only 9 of the 39 residues in the loop are identical in *Synechocystis* sp. PCC 6803, and regions of the loop generally cannot be exchanged between the two proteins (*16*). This suggests that the CD loop region helps to define the

† This work was supported by a grant from the National Institutes of Health to W.F.J.V. (GM 51556). A.T.K. was supported by a Graduate Research Training (GRT) grant from the National Science Foundation (DGE-9553456).

* Corresponding author. Tel: (480) 965-3698. Fax: (480) 965-6899. E-mail: wim@asu.edu.

[1] Abbreviations: Chl, chlorophyll; DCMU, 3-(3,4-dichlorophenyl)-1,1-dimethylurea; DMBQ, 2,5-dimethyl-*p*-benzoquinone; EPR, electron paramagnetic resonance; F_o, constant fluorescence; F_m, maximal fluorescence; F_v, variable fluorescence; OEC, oxygen-evolving complex; P680, primary donor of PS II; PS I, photosystem I; PS II, photosystem II; Q_A, primary electron accepting quinone in PS II; Y_D, tyrosine$_D$ (Tyr160 of the D2 protein), an accessory electron donor in PS II; Y_Z, tyrosine$_Z$ (Tyr161 of the D1 protein), the immediate electron donor to P680.

10.1021/bi002772d CCC: $20.00
Published on Web 03/08/2001

structural and functional environment around Y_Z and Y_D.

The CD lumenal loop of the D2 protein contains several amino acid residues that interact with Y_D and/or P680, indicating its close proximity to the primary donor. His189 is within H-bonding distance of Y_D and is the proton acceptor when Y_D is oxidized to the strongly acidic Y_D^+ (*6*, *9*, *10*, *17*). When mutated, Gln164 alters the electron paramagnetic resonance (EPR) signal of Y_D^{ox} (*7*), indicating a close interaction between the two residues. Arg180, located in the α-helical portion of the loop, affects both Y_D and P680 function (*18*). The Arg180 residue possibly serves as a bifunctional group, allowing stable Y_D oxidation and acting as a ligand to an accessory chlorophyll that is the homologue of the accessory pigment in the reaction center of purple bacteria. In contrast to the situation in purple bacteria, this accessory chlorophyll in PS II may be part of P680 as P680 appears to be a multimer of weakly coupled pigments (*19*, *20*). These pigments include four chlorophylls: the two chlorophylls that are homologous to the "special pair" in the reaction center of purple bacteria and liganded to His198 and His197 of D1 and D2, respectively, and two accessory chlorophylls between the special pair homologues and the two pheophytins. The accessory chlorophyll on the D2 side appears to interact closely with Arg180.

In addition to the His189, Arg180, and Gln164 residues, computer models based on the purple bacterial reaction center have suggested important roles for several other residues in the CD loop of D2. Trp191 was proposed to provide ring-stacking forces to a central chlorophyll of P680 (the one for which His197 of D2 may be a ligand) while Phe179 was thought to provide the similar stacking forces to the accessory chlorophyll (*14*, *15*) that most likely is associated with Arg180 (*18*).

Recently, our group conducted a comprehensive combinatorial mutagenesis of the CD lumenal loop of D2 in *Synechocystis* sp. PCC 6803 leading to the development of sets of functional mutants in this region (*16*). However, characterization of the functional changes resulting from the combinatorial mutagenesis is required to understand the roles of specific residues and domains in this region. A study on charge recombination pathways involving some of the mutants to be analyzed here has appeared recently (*21*). In the current paper results will be presented on PS II properties in a set of combinatorial mutants with changes at the C-terminal end of the CD loop. Since this region may interact with P680, with Y_D, and indirectly with the OEC, the mutants were screened to detect alterations in the function of components at the donor side of PS II. Several residues including Trp191 were found to affect P680 properties, and surprisingly, many changes in this region greatly decreased the apparent affinity of the OEC for Cl^-, emphasizing the effect of this region on the properties of the OEC.

MATERIALS AND METHODS

Photoautotrophic Strains. The *Synechocystis* sp. PCC 6803 combinatorial mutant strains used in this study were developed using an M13-based combinatorial mutagenesis technique that was previously described (*16*). A total of 34 photoautotrophic combinatorial mutants carrying random sequences in the eight amino acid region around His189 in D2 (Gly187−Asn194) were isolated, and nine of these were analyzed in this study. The primary amino acid sequences of the mutagenized region in these nine mutants are listed in Table 1. In five of these nine combinatorial mutants Trp191, the residue present in the wild type at this position, was restored (Table 1) using M13-based site-directed mutagenesis with the original combinatorial mutants as the template (*16*). In addition, for two combinatorial mutants the wild-type residues at positions 191 and 192 (Trp and Thr, respectively) were restored by similar site-directed mutagenesis. These sequences are also listed in Table 1.

Table 1: Amino Acid Sequences in the C-Terminal Part of the CD Lumenal Loop Region of the D2 Protein (Gly187−Asn194) for the *Synechocystis* sp. PCC 6803 Strains Used in This Study[a]

strain	sequence 187							194
wild type	G	F	**H**	N	W	T	L	N
Combinatorial Strains								
C8-1	G	A	**H**	A	V	L	Q	L
C8-2	A	F	**H**	G	F	I	M	Q
C8-4	S	F	**H**	N	F	L	L	V
C8-7	G	F	**H**	G	F	A	D	S
C8-10	A	S	**H**	C	I	V	C	L
C8-14	S	V	**H**	A	M	T	M	Y
C8-22	A	L	**H**	G	V	T	N	M
C8-23	G	M	**H**	G	I	A	V	S
C8-25	V	F	**H**	Q	W	S	L	H
Combinatorial Strains with Restored Trp191								
C8-2W191	A	F	**H**	G	*W*	I	M	Q
C8-4W191	S	F	**H**	N	*W*	L	L	V
C8-7W191	G	F	**H**	G	*W*	A	D	S
C8-14W191	S	V	**H**	A	*W*	T	M	Y
C8-22W191	A	L	**H**	G	*W*	T	N	M
Combinatorial Strains with Restored Trp191 and Thr192								
C8-7W191T192	G	F	**H**	G	*W*	*T*	D	S
C8-23W191T192	G	M	**H**	G	*W*	*T*	V	S
Site-Directed Mutant Strains								
F188E	G	**E**	**H**	N	W	T	L	N
H189Q	G	F	**Q**	N	W	T	L	N
W191L	G	F	**H**	N	**L**	T	L	N
T192A	G	F	**H**	N	W	**A**	L	N
W191L/T192A	G	F	**H**	N	**L**	**A**	L	N

[a] His189 is in boldface in all sequences. Tryptophan (W) and threonine (T) are italicized in combinatorial sequences if they were restored at the 191 and 192 positions by subsequent mutagenesis. For site-directed mutant strains, the mutated residue(s) has (have) been bolded and underlined.

In addition to the combinatorial mutants tested, several photoautotrophic site-directed mutants (four single-site mutants and one double mutant) were also examined (Table 1). The H189Q mutant has been previously described (*17*). The F188E, W191L, T192A, and W191L/T192A mutants were developed using previously described site-directed mutagenesis techniques (*22*).

PS I-less Strains. Removal of photosystem I (PS I) from *Synechocystis* sp. PCC 6803 strains results in a 6-fold decrease in the amount of chlorophyll per cell (*23*), greatly simplifying evaluations of PS II parameters such as variable fluorescence and the shape and intensity of Y_D^{ox} EPR signals. Therefore, all mutants were transformed into a PS I-less background by transformation of the PS I-less/*psb*DIC$^-$/*psb*DII$^-$ strain (*24*) with the mutant genomic DNA. Since all mutants carry a kanamycin resistance cassette downstream of the *psb*DIC operon, transformant selection was based on kanamycin resistance.

Growth Conditions. PS I-containing wild type and mutant strains of *Synechocystis* sp. PCC 6803 were grown in liquid BG-11 medium (*25*) at 30 °C at 40−50 μmol of photons m^{-2} s^{-1}. These photoautotrophic strains were segregated and maintained at ∼20−30 μmol of photons m^{-2} s^{-1} on solid BG11 medium supplemented with 1.5% (w/v) agar, 0.3% (w/v) sodium thiosulfate, and 10 mM TES−NaOH buffer (pH 8.2). PS I-less strains were grown at ∼5 μmol of photons m^{-2} s^{-1} in modified BG-11 medium (containing 4.5 mM ammonium nitrate and 13.2 mM $NaNO_3$ as fixed nitrogen sources and supplemented with 10 mM glucose and 10 mM TES−NaOH buffer, pH 8.2). Segregation of PS I-less strains was done on modified solid BG-11 medium containing 10 mM glucose and 5 μg/mL kanamycin. Upon segregation the kanamycin concentration was increased to 25 μg/mL for maintenance purposes. All liquid cultures in volumes less than 1 L were grown on a rotary shaker while larger culture volumes were bubbled with air.

Calcium (Ca^{2+}) and chloride (Cl^-) depletion medium for nutrient deprivation experiments was prepared as previously described (*26*). For depletion of these ions, PS I-containing mutants were grown in liquid Ca^{2+}/Cl^--less BG-11 medium where NaCl replaced $CaCl_2$ for Ca^{2+} depletion and $CaSO_4$ and $MnSO_4$ replaced $CaCl_2$ and $MnCl_2$ for Cl^- depletion. Cultures were supplemented with 5 mM glucose and grown for 2−4 subcultures until oxygen evolution rates showed no further decrease (*26*). Depleted cultures were concentrated 10-fold and subcultured, in the absence of glucose (photoautotrophic growth conditions), into Ca^{2+}-less and Cl^--less BG-11 medium as well as BG-11 medium containing standard amounts of calcium and chloride (0.25 mM Ca^{2+}- and 0.5 mM Cl^-). Stock solutions of 0.01 M $CaSO_4$ and 0.1 M KCl were used to add desired concentrations of Ca^{2+} or Cl^-, respectively, to the appropriate depletion medium to further quantitate the Ca^{2+} or Cl^- requirement for photoautotrophic growth of each mutant tested.

Oxygen Evolution. For oxygen evolution measurements, cultures were grown in liquid medium to OD_{730} = 0.4−1.0 and concentrated in fresh TES-buffered BG-11 medium to a chlorophyll concentration of 3−10 μg/mL as determined by absorption at 663 nm after chlorophyll extraction from cells in 100% methanol. Oxygen evolution was measured in PS I-containing mutants in the presence of 0.5 mM $K_3Fe(CN)_6$ and 0.3 mM DMBQ (2,5-dimethyl-*p*-benzoquinone) at 25 °C with a Clark-type electrode. Samples were illuminated with saturating light of ∼2000−3000 μmol of photons m^{-2} s^{-1} which had been passed through an orange filter, eliminating wavelengths <570 nm.

Variable Fluorescence Induction and Decay Measurements. Chlorophyll *a* variable fluorescence induction and decay measurements, reflecting kinetics of Q_A reduction and Q_A^- reoxidation, respectively, were measured using a PAM fluorometer (Walz, Effeltrich, Germany) and recorded using FIP fluorescence software (Q_A Data, Turku, Finland). The maximum intensity of the measuring and actinic light was at about 650 nm, at which wavelength both chlorophyll and phycobilisomes absorb. Cell suspensions of PS I-less mutants were grown to OD_{730} = 0.4−1.0 (corresponding to about 0.3−1 μg of Chl/mL) and measured directly in TES-buffered modified BG-11 plus 5 mM glucose in the presence of 50 μM DCMU. To measure the intensities of initial (F_o, PS II centers are open), maximal (F_m, PS II centers are closed), and variable ($F_v = F_m - F_o$) fluorescence, the cell suspension was incubated for 2 min in darkness and then illuminated for up to 3 s, during which period the maximum fluorescence signal (F_m) was reached. To measure the decay of variable fluorescence, the samples were illuminated either with a saturating single-turnover Xe flash or with a 400 ms pulse of continuous red light (maximal intensity around 650 nm; light intensity, 30 μmol of photons m^{-2} s^{-1}) to reduce Q_A. Then the decrease in the fluorescence yield as probed by weak modulated light (1.6 kHz) was recorded.

Picosecond Fluorescence Decay. Time-resolved picosecond fluorescence decays of intact cells of PS I-less strains were measured in a single-photon-timing spectrometer essentially as described by Bittersmann and Vermaas (*27*). Large volumes (1.4 L) of PS I-less cyanobacterial mutant cultures were grown to similar OD_{730} and chlorophyll concentrations as for the experiments to monitor variable fluorescence induction and decay. Cells were either dark adapted (open centers) or illuminated in the presence of 10 μM DCMU (closed centers) and pumped through a flow cuvette at a rate of about 10 mL/s. Cells in the flow cuvette were excited with 5−15 ps laser pulses (4.3 MHz) at 600 nm, absorbed by phycobilisomes, and the fluorescence was detected at 680 nm with a microchannel plate photomultiplier. The full width at half-maximum of the instrument response function in this configuration was 60−75 ps as measured with a Ludox scattering sample.

Thylakoid Membrane Preparation for EPR Studies. The method used to prepare thylakoid membranes of PS I-less strains for EPR studies has been previously described (*28*). To chelate aqueous Mn^{2+}, the thylakoid buffer was supplemented with 10 mM EDTA (pH 8.0). Cells were broken in microfuge tubes using a BeadBeater. The final pellet was resuspended in cold thylakoid buffer (25 mM Hepes−NaOH, pH 7.0, 5 mM $MgCl_2$, 15 mM $CaCl_2$, 15% glycerol, 0.5% DMSO, and 10 mM EDTA) to a final chlorophyll concentration of 70−300 μg/mL. Approximately 0.5 mL of the final preparation was transferred to an EPR tube, dark adapted for 30−60 min, then frozen in darkness, and stored in liquid nitrogen until used.

EPR Spectroscopy. To observe the properties of Y_D^{ox}, difference spectra were determined using thylakoid membrane preparations of PS I-less mutant strains. EPR spectra of dark-adapted samples were recorded at 125 K using a Bruker Elexsys E580 spectrometer. Light spectra were recorded after the samples had been illuminated for 10 min at −20 °C and returned to liquid nitrogen while illuminating. Using this method we generally find an ∼30% increase in the Y_D^{ox} signal for wild-type PS I-less *Synechocystis* sp. PCC 6803 reflecting oxidation of Y_D in the sample. Difference spectra were determined by a light minus dark subtraction of the two spectra. EPR experimental conditions for all spectra were as follows: sample temperature 125 K, microwave frequency ∼9.4 GHz, microwave power 0.5 mW, magnetic field modulation frequency 100 kHz, and magnetic field modulation amplitude 0.3 mT. A typical spectrum represents data averaging of 32 scans with a time constant of 82 ms, scan time of 84 s, and a scan rate of 0.125 mT/s.

RESULTS

As the result of comprehensive combinatorial mutagenesis of the CD lumenal loop of the D2 protein in *Synechocystis*

Table 2: Variable Fluorescence Yield and Charge Recombination Rates in Combinatorial and Site-Directed Mutants[a,b]

strain	F_v/F_m	$t_{1/2}$ Q_A^- reoxidation (ms)[c]
wild type	0.64	211
C8-1	0.58	38
C8-2	0.50	59
C8-2W191	0.64	131
C8-4	0.34	64
C8-4W191	0.62	192
C8-7	0.54	33
C8-7W191	0.70	94
C8-7W191T192	0.70	175
C8-10	0.56	79
C8-14	0.59	112
C8-14W191	0.60	326
C8-22	0.23	106
C8-22W191	0.61	231
C8-23	0.49	48
C8-23W191T192	0.66	223
C8-25	0.57	230
F188E	0.66	121
H189Q	0.64	126
W191L	0.63	71
T192A	0.66	131
W191L/T192A	0.60	47

[a] In some of the combinatorial mutants a Trp residue at position 191 and/or a Thr residue at position 192 had been restored. The amount of variable fluorescence relative to the total fluorescence yield (F_v/F_m) and the half-time ($t_{1/2}$) of the loss of variable fluorescence (representing Q_A^- reoxidation) were measured after illumination of samples in the presence of DCMU. All measurements were done on strains lacking PS I. [b] Reported values are reproducible within 20% and represent averages of at least two but typically three independent measurements. [c] Reported data are from samples exposed to a 400 ms flash. Exposure of samples to a single-turnover flash showed similar results.

sp. PCC 6803, 34 combinatorial mutants were isolated in the eight amino acid region near the C-terminal end of the CD loop (Gly187−Asn194) (*16*). Since this region of the CD loop is close to P680 [according to models (*14*, *15*) particularly to one of the central chlorophylls to which His197 of D2 is thought to be a ligand], a preliminary screen of the 34 strains consisted of monitoring variable fluorescence induction and rate of decay after illumination in the presence of DCMU. These studies were done on mutants in a PS I-less background, as the variable fluorescence yield is large in the absence of PS I. The majority of the strains showed an increased rate of Q_A^- reoxidation in the presence of DCMU, reflecting a change in the charge recombination rate between Q_A^- and the donor side. Two strains, C8-4 and C8-22, showed a reduction in the amplitude of variable fluorescence relative to the total chlorophyll fluorescence (F_v/F_m ratio; Table 2 and Figure 1). In addition to fluorescence testing, the mutants were screened for alterations in the ion requirement of the OEC by measuring growth rates and oxygen evolution after Ca^{2+} or Cl^- deprivation. Many of the mutants required the presence of high chloride concentrations in the medium for photoautotrophic function, while two mutants (C8-10 and C8-23) also demonstrated the need for an increased calcium concentration.

On the basis of the results of the preliminary fluorescence and ion requirement studies, nine strains representing the various phenotypes were selected for further testing (Table 1). Among these nine are those strains that showed the most severe alterations. In addition to these combinatorial strains, we analyzed several site-directed mutants with alterations

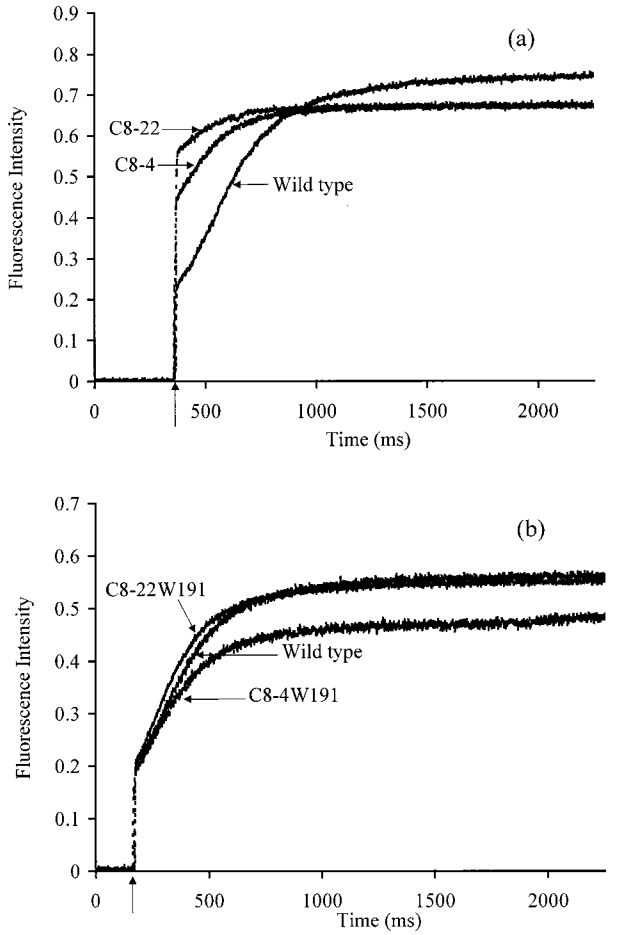

FIGURE 1: Fluorescence induction curves in the presence of DCMU for (a) wild type, C8-4, and C8-22 and (b) wild type, C8-4W191, and C8-22W191. All strains were in a PS I-less background, and the cell densities were comparable. The intensity of the excitation light was maximal around 650 nm. The arrows indicate the point at which a sample was exposed to light.

in this region. These were F188E, H189Q, W191L, T192A, and W191L/T192A (Table 1). By analyzing these single and double site-directed mutants in parallel with the combinatorial mutants, more accurate insight could be obtained regarding which residues were mainly associated with which phenotype.

Q_A^- Reoxidation Kinetics. The half-time of Q_A^- reoxidation in the nine combinatorial mutants along with the site-directed strains is shown in Table 2. The rate of Q_A^- reoxidation by recombination with the donor side of PS II was 2−5 times faster than that of wild type in all but one of the 34 combinatorial mutants tested (C8-25). Interestingly, C8-25 was the only combinatorial mutant to retain Trp191 (*16*).

Indeed, mutation of just Trp191 already has a sizable effect on the Q_A^- reoxidation kinetics, as evidenced by the 3-fold decrease of the half-time of Q_A^- oxidation in the W191L mutant. However, nearby residues also have a significant effect on the charge recombination kinetics with mutation of Phe188, His189, and Thr192 each causing a 2-fold increase in the charge recombination rate. In the case of the Thr192 mutation the effect is additive to that of the Trp191 mutation since the W191L/T192A double mutation destabilizes Q_A^- (in the presence of DCMU) by a factor of 4−5 relative to wild type. The normal Q_A^- oxidation kinetics in

C8-25, which retains the wild-type residues at positions 188, 189, and 191 along with a conservative mutation at position 192 (T192S), together with fast charge recombination in the site-directed mutants at these positions, suggests that these four residues are most important in this domain for determining the charge recombination rate.

Restoration of Trp191. To test whether Trp191 has as large an impact on charge recombination in the combinatorial mutants as it does in the W191L mutant, five of the combinatorial mutants (C8-2, C8-4, C8-7, C8-14, and C8-22) were mutated once more to recreate Trp191 in these mutants (Table 1). The resulting mutants were named C8-2W191, C8-4W191, C8-7W191, C8-14W191, and C8-22W191, respectively. In addition, in two strains, C8-7 and C8-23, both Trp191 and Thr192 were restored. The resulting strains were named C8-7W191T192 and C8-23W191T192.

Table 2 summarizes the results of the comparative analysis of mutants before and after restoration of Trp at position 191. Indeed, restoration of Trp at the 191 position in the combinatorial background in all selected mutants slowed the charge recombination rate by at least 2-fold. In the case of C8-14, the fluorescence yield decay rate slowed 3-fold, making the rate of Q_A^- reoxidation ~50% slower than that of wild type. Interestingly, the restoration of both Trp191 and Thr192 in the C8-7 and C8-23 combinatorial background returned the charge recombination rate to at or near wild-type values, providing further evidence of the composite effect of residues 191 and 192 on charge recombination rates.

Mutants with Reduced F_v/F_m Ratio. Two out of the original 34 mutants tested, C8-4 and C8-22, showed a decreased variable fluorescence yield (Table 2). This phenotype was most pronounced in the C8-22 mutant with a F_v/F_m ratio three times lower than for wild type and with an increased F_o. An example of fluorescence induction curves is presented in Figure 1a. Reintroduction of Trp191 into the C8-4 and C8-22 combinatorial backgrounds yielded induction curves similar to those of wild type (Figure 1b). As these measurements were performed in PS I-less strains, a change in the PS II/PS I ratio can be excluded as a cause for this large change. Instead, these mutants may have an alteration in excitation trapping and/or charge separation parameters.

To elucidate the cause of the unusually low F_v/F_m ratio in C8-22, time-resolved fluorescence decay measurements in the pico- to nanosecond time domain were performed (Figure 2). The excitation wavelength was 600 nm, absorbed primarily by phycobilisomes. The fluorescence lifetime in the C8-22 strain was considerably longer than in the control when PS II centers were open but somewhat shorter when the centers were closed. Indeed, fitting of the fluorescence decay curves with a sum of exponential components showed the fast phase of decay in open centers to be significantly slower in the C8-22 strain than in the control (500 versus 230 ps; Table 3). This agrees with the increased F_o fluorescence yield detected by the fluorescence induction measurements (Figure 1). An explanation consistent with these observations is that the excitation trapping efficiency in the C8-22 mutant is significantly lower than in PS II with the wild-type CD loop sequence. The C8-22W191 mutant and the W191L strain showed rather normal fluorescence lifetimes. It should be emphasized that the fluorescence decay components listed in Table 3 represent the overall excitation lifetime in intact cells, which is a composite of excitation transfer and trapping events. Therefore, this lifetime does not directly reflect the rate of a specific exciton or electron-transfer step.

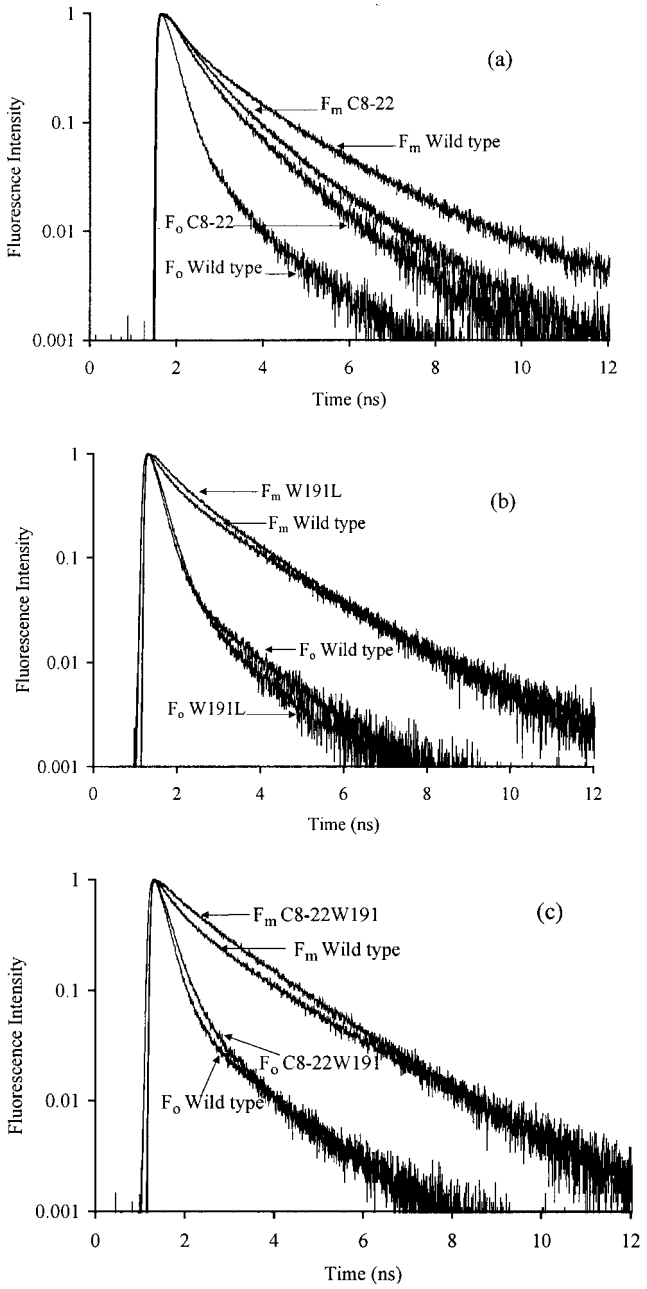

FIGURE 2: Picosecond fluorescence decay curves for PS I-less *Synechocystis* sp. PCC 6803 strains C8-22 (a), W191L (b), and C8-22W191 (c) as compared to wild type with PS II centers open (F_o) or closed (F_m). Samples were excited with 600 nm light, and emission was detected at 680 nm.

Tyr160 Properties. To determine if the combinatorial mutations significantly altered the environment around Tyr160 (Y_D), continuous wave EPR spectra of thylakoids from wild type and the C8-4 and C8-22 strains were determined. These two mutants were chosen because they displayed the most severe alterations with regard to the fluorescence properties. Figure 3 shows that neither the stability of Y_D^{ox} nor its electron spin distribution was radically altered in the combinatorial mutants. Both mutants have line shapes of the difference spectra similar to those of wild type. However, C8-22 appears to have a lower yield of Y_D^{ox} upon illumination than wild type. The amplitude of the

Table 3: Fluorescence Lifetimes and Relative Amplitudes of *Synechocystis* sp. PCC 6803 Wild Type, Combinatorial Mutants C8-22 and C8-22W191, and Site-Directed Mutant W191L[a]

		wild type			C8-22			W191L			C8-22W191		
F_o	lifetime (ns)	0.23	1.5		0.50	1.4		0.26	1.4		0.27	1.3	
	amplitude	0.96	0.04		0.77	0.23		0.97	0.03		0.95	0.05	
F_m	lifetime (ns)	0.35	1.3	2.6	0.55	1.3	3.1	0.46	1.4	3.7	0.46	1.5	2.9
	amplitude	0.52	0.39	0.09	0.67	0.31	0.02	0.41	0.56	0.03	0.31	0.65	0.04

[a] For open centers (F_o) two lifetime components provided an adequate fit. For closed centers (F_m) a three-component fit was better.

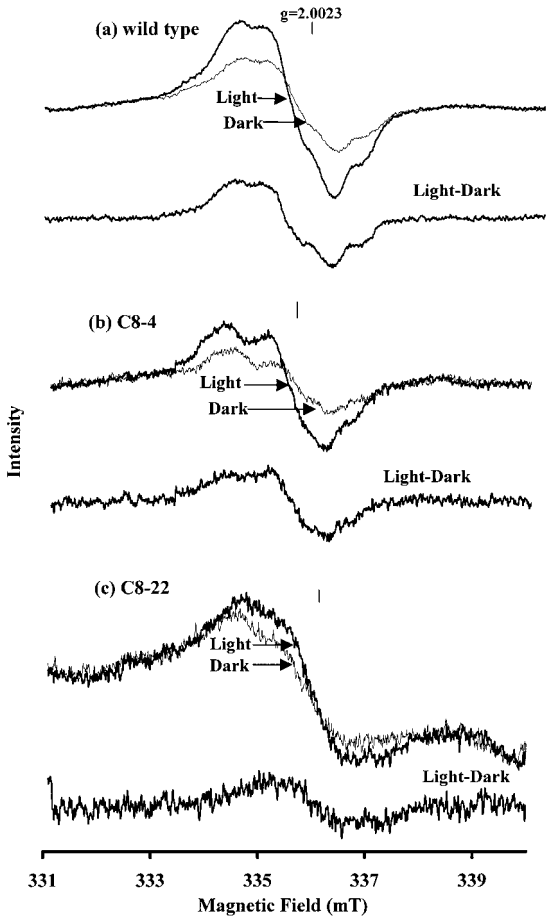

FIGURE 3: Light, dark, and light minus dark difference continuous wave EPR spectra of thylakoids from (a) wild type, (b) C8-4, and (c) C8-22. The vertical line at the top of each spectrum corresponds to $g_e = 2.0023$. The g-values for the difference spectra were within normal range for the Y_D^{ox} radical: wild type = 2.0055, C8-4 = 2.0039, and C8-22 = 2.0039. The chlorophyll concentrations were 298 μg/mL for the wild type, 95 μg/mL for C8-4, and 74 μg/mL for C8-22. All other conditions are listed in Materials and Methods.

light-induced spectra is similar for all three samples relative to the chlorophyll concentration, but C8-22 has approximately 50% more dark signal than wild type or C8-4. This indicates that the radical in this mutant may be somewhat more stable in the dark.

Nutrient Deprivation Studies. Oxygen evolution via the manganese cluster of PS II requires the presence of calcium and chloride cofactors. Initial studies of the 34 combinatorial mutants showed that all but eight could not survive photoautotrophically in conditions of chloride depletion that was not detrimental to wild type, and two mutants, C8-10 and C8-23, were sensitive to calcium depletion as well. Data on photoautotrophic growth rates, oxygen evolution, and growth rates under conditions of calcium or chloride depletion are presented in Table 4 for the mutants that were selected for further analysis. Several of the Trp191 restoration mutants as well as the site-directed mutants were also included in this analysis. Note that remaining photautotrophic growth in the absence of added Ca^{2+} or Cl^- is an indication of contamination of water or chemicals with these ions. However, these contaminant levels were similar for all strains as they were propagated in identical batches of medium.

Table 4: Growth Characteristics of Selected Strains under Normal Photoautotrophic Conditions with and without Depletion of Cl^- and Ca^{2+} [a]

strains	doubling time (h)	O_2 evolution [μmol of O_2/(mg of Chl·h)]	growth rate after depletion (% of rate in normal BG-11)	
			Cl depleted	Ca depleted
wild type	11.9 ± 1.9	332 ± 58	67	100
C8-1	14.7 ± 1.8	293 ± 59	0	82
C8-2	14.6 ± 2.5	250 ± 50	0	77
C8-4	14.1 ± 1.6	276 ± 32	0	90
C8-4W191	14.8 ± 3.4	281 ± 84	0	88
C8-7	14.0 ± 1.9	213 ± 71	14	89
C8-7W191T192	12.0 ± 1.3	304 ± 68	33	86
C8-10	19.9 ± 2.8	276 ± 89	0	0
C8-14	18.4 ± 2.9	293 ± 73	0	98
C8-22	16.5 ± 3.1	252 ± 79	0	72
C8-22W191	14.7 ± 1.7	253 ± 50	0	91
C8-23	24.1 ± 3.5	192 ± 54	0	0
C8-23W191T192	12.6 ± 0.9	326 ± 30	0	84
F188E	15.8 ± 4.3	311 ± 59	43	84
H189Q	21.0 ± 2.7	376 ± 65	0	100
W191L	13.4 ± 0.9	308 ± 53	67	87
T192A	15.2 ± 2.7	354 ± 64	50	91
W191L/T192A	17.1 ± 1.3	352 ± 71	0	98

[a] The combinatorial mutants along with their Trp191 restoration counterparts are shown first followed by the site-directed mutants. All data presented are the result of at least two but typically three independent measurements.

The majority of the strains could not grow photoautotropically in the absence of added chloride. To further quantitate the calcium and chloride requirements, selected strains were depleted of both cofactors, and photoautotrophic growth rates were then determined for each mutant in media containing differing concentrations of each nutrient (Table 5). All strains (including wild type) showed some degree of photoautotrophic growth rate impairment when the chloride concentration of the medium decreased to 0.1 mM, 20% of the normal concentration. However, unlike wild type, most of the combinatorial strains could not survive when the chloride concentration in the medium was 0.01 mM, 2% of the normal concentration. C8-23 was the most severely affected, being unable to survive at 0.1 mM chloride.

Three of the site-directed mutants (F188E, W191L, and T192A) showed the same pattern as wild type with minor

Table 5: Photoautotrophic Doubling Times (h) of Selected Combinatorial Strains, Strains in Which Trp191 and/or Thr192 Have (Has) Been Restored, and Site-Directed Mutant Strains under Various Chloride or Calcium Depletion Conditions[a]

	normal BG-11	chloride depletion				calcium depletion	
strains	0.5 mM Cl^-, 0.25 mM Ca^{2+}	0.1 mM Cl^-, 0.25 mM Ca^{2+}	0.01 mM Cl^-, 0.25 mM Ca^{2+}	0.001 mM Cl^-, 0.25 mM Ca^{2+}	Cl^--less, 0.25 mM Ca^{2+}	0.5 mM Cl^-, 0.025 mM Ca^{2+}	0.5 mM Cl^-, Ca^{2+}-less
wild type	12 ± 2	14 ± 1	18 ± 2	19 ± 3	18 ± 2	13 ± 1	12 ± 1
C8-4	14 ± 2	18 ± 1	NG[b]	NG	NG	16	16 ± 1
C8-4W191	15 ± 3	16 ± 1	77	NG	NG	16	17 ± 1
C8-7	14 ± 2	17 ±1	36 ± 12	67	98	16 ± 4	16 ± 4
C8-7W191T192	12 ± 1	16	22 ± 1	35 ± 3	36 ± 10	10	14 ± 1
C8-22	17 ± 3	23 ± 3	NG	NG	NG	18 ± 3	23 ± 4
C8-22W191	15 ± 2	22	NG	NG	NG	17	16 ± 1
C8-23	24 ± 4	NG	NG	NG	NG	NG	NG
C8-23W191T192	13 ± 1	18 ± 1	NG	NG	NG	13 ± 1	15 ± 2
F188E	16 ± 4	20 ± 6	30 ± 8	36 ±10	37 ± 6	18 ± 5	19 ± 6
H189Q	21 ± 3	28	73	NG	NG	18	20 ± 1
T192A	15 ± 3	18 ± 2	27 ± 6	27 ± 5	31 ± 8	17 ± 2	17 ± 1
W191L	13 ± 1	17.1 ± 2	19.0 ± 2	19.7 ± 3	20 ± 3	15 ± 2	16 ± 3
W191L/T192A	18 ± 1	19 ± 1	44 ± 1	NG	NG	18	18 ± 0

[a] Following Ca^{2+}/Cl^- depletion the doubling times were determined in normal BG-11 medium (first column of data) or in BG-11 medium containing decreased concentrations of Ca^{2+} or Cl^-. Cl^--less and Ca^{2+}-less indicate that no Cl^- or Ca^{2+} was added. Where no standard deviation is given, the doubling time at the indicated concentration was determined only once, but other data were obtained at slightly different Ca^{2+} and Cl^- concentrations that support the reported data. [b] NG = no growth under the indicated conditions.

growth impairment at 0.1 mM chloride but without additional effect at lower chloride concentrations. However, H189Q and the double mutant W191L/T192A did not grow photoautotropically when 1 μM chloride was added to Cl^--depleted cells and grew slowly with 10 μM chloride. H189Q grew at half its normal photoautotrophic rate at 50 μM added chloride (data not shown). W191L/T192A showed only slightly better tolerance for chloride depletion than H189Q, whereas both single mutants, W191L and T192A, did not show a clear Cl^-effect. The W191L/T192A strain maintained the ability to grow at about half its normal photoautotrophic rate at 10 μM chloride but was unable to survive when the added chloride concentration was an order of magnitude lower.

Except in the case of C8-23, quantification of the calcium requirement for the combinatorial and site-directed mutants indicated no or only mild impairment in the presence of 25 μM or less calcium (Table 5). The C8-23 strain did not grow photoautotrophically even in the presence of 50 μM Ca^{2+} (data not shown).

DISCUSSION

Combinatorial mutagenesis of the C-terminal end of the CD lumenal loop in D2 protein of PS II in *Synechocystis* sp. PCC 6803 has led to the isolation of functional mutants that display an intriguing range of effects on the donor side of PS II. Observed changes in the fluorescence parameters may indicate an alteration of the redox behavior of one of the PS II components. Additionally, changes affecting ion requirements for normal oxygen evolution have been observed that may indicate a closer involvement of this region in determining the properties of the water-splitting process than previously thought.

Mutational Effects on Redox Properties of PS II. A significant alteration seen in this set of combinatorial mutants with regard to fluorescence parameters is the increased rate of Q_A^- reoxidation due to faster charge recombination between Q_A^- and the donor side of PS II. Thus far, most mutations on the donor side of PS II that demonstrate a faster rate of Q_A^- reoxidation seem to reflect an increase in concentration of $P680^+$ that could be attributable to a change in the properties of P680, Y_Z, and/or the S states of the OEC. The Y161P mutant that lacked a photooxidizable Y_Z radical and was incapable of photoautotrophic growth showed an 80-fold increased charge recombination rate compared to wild type due to a lack of donor-side electron donation to $P680^+$ (*2*). Several D1 mutants with donor-side changes show impaired photoautotrophic growth along with faster rates of charge recombination presumably due to a loss of photooxidizable Mn ions (*29*, *30*). The combinatorial mutants analyzed in the present study maintain normal and stable oxygen evolution and grow well photoautotrophically. We interpret this to suggest that the induced changes are not likely to radically affect the redox properties of Y_Z or the OEC but instead may alter the properties of the $P680/P680^+$ redox couple directly.

Several factors affect the value of the midpoint potential of the primary donor in photosynthetic systems. One is the presence of hydrogen bonds to the reaction center pigments (*31*). Previous studies on D2 CD loop mutants have demonstrated charge recombination phenotypes that were interpreted to represent an alteration in the $P680/P680^+$ redox midpoint potential. Site-directed Arg180 mutants showed drastic alterations in the half-time of Q_A^- reoxidation, suggesting that this residue is closely involved in the stability and charge distribution around P680 as well as possibly stabilizing Y_D^{ox} (*18*). This was interpreted to indicate a stabilization of $P680^+$, thus altering steady-state conditions to favor a faster rate of charge recombination (*18*). In fact, the protein environment around P680, in particular the presence of specific residues such as Arg180, has been proposed to be instrumental in determining the high oxidizing potential of this primary donor (*32*).

In selected combinatorial mutants from other regions of the CD loop the charge recombination rate changes were accompanied by changes in thermoluminescence yield that were also interpreted to result from a midpoint potential shift of the $P680/P680^+$ redox couple (*21*). Unlike the Arg180 mutants and combinatorial mutants in other regions of the

CD loop that appear to affect Y_D (*18*, *21*), this redox-active Tyr is essentially normal in C8-4 and C8-22 that are representative of mutants with the most severe phenotypic changes in the region. Consequently, faster charge recombination in the combinatorial mutants presented here is unlikely to result from changes in Y_D properties.

In the region that is considered in this study, Trp191 in particular had a significant impact on the charge recombination phenotype. The rate of Q_A^- reoxidation was changed by a factor of 2−3 as a function of removal or recreation of Trp191. On the basis of the sequence alignment of D2 with the M subunit of the purple bacterial reaction center Trp191 is homologous to Leu194 (M), which is located within 6 Å of the bacteriochlorophyll special pair (*33*). This distance may be shortened when replacing Leu by the larger Trp. Indeed, PS II models show Trp191 to be within 3.5−4.5 Å of the central P680 chlorophyll (*14*, *15*) that is presumed to have His197 of D2 as a ligand. Trp191 may provide ring-stacking forces for proper orientation of the chlorophyll (*14*, *15*), and Trp191 and this chlorophyll of P680 even may be in contact via weak hydrogen bonds (*15*). This proposed orientation of Trp191 in the PS II reaction center and the potential hydrogen bonding indeed would support the idea of a change in the P680/$P680^+$ redox potential due to the removal of Trp191 from the region. Moreover, a nonliganding Trp residue 3.6 Å from a heme cofactor in a perpendicular orientation was found to induce significant changes in the midpoint redox potential of this heme (*34*), indicating that even a nonliganding residue may strongly influence the redox properties of protein-bound porphyrin cofactors.

It is interesting that even in the presence of Trp191 single-site mutations at positions 188, 189, and 192 resulted in a 2-fold increase in the charge recombination rate. While His189 affected Y_D properties, the other two positions are not known to play a significant role. Perhaps mutations at positions 188 and 192 alter the orientation of Trp191 such that electronic interaction between Trp191 and chlorophyll is decreased. In line with this argument is the observation that reintroduction of Trp191 alone does not completely revert the charge recombination kinetics to those in the control whereas reintroduction of both Trp191 and Thr192 slowed charge recombination to essentially the control level in the two combinatorial backgrounds in which they were restored.

Mutational Effects on Fluorescence Lifetimes. Two mutants analyzed in this study, C8-4 and C8-22, showed a decrease in variable fluorescence yield primarily due to a long fluorescence lifetime in open centers leading to an increased F_o level. Interestingly, upon reintroduction of Trp191 the fluorescence lifetime returned to normal even though the W191L mutant shows that Trp191 is not required for a normal fluorescence lifetime. According to the model of excitation transfer and trapping suggested by Schatz et al. (*35*), the longer lifetime of fluorescence in open centers may have two causes. First, the reaction center may have a lower trapping efficiency due to a slower rate of primary charge separation between P680 and pheophytin relative to the excitation transfer back to the antenna. Alternatively, the charge recombination rate between $P680^+$ and $Pheo^-$ may have increased, resulting in re-formation of excited chlorophyll by a faster back-reaction rate or, more probably, a slower transfer from $Pheo^-$ to Q_A. These two possibilities cannot be distinguished on the basis of the present results. However, because of the close proximity of the mutations to P680 we favor the first option.

While the charge recombination kinetics were altered in most of the combinatorial mutants, the F_o level was increased in only two of the mutants. This implies that the changes in midpoint potential and the overall trapping efficiency are independent parameters, as has also been observed in the reaction center from purple bacteria (*31*). Interestingly, both a certain combination in the Gly187−Asn194 region (as is present in C8-4 and C8-22) and the absence of Trp191 are needed to observe the increased F_o and decreased overall trapping efficiency. Reintroduction of Trp191 or having one of the 32 other combinatorial mutations led to fluorescence lifetimes comparable to those in the control. However, comparing the sequence in C8-4 and C8-22 versus that in the other mutants does not identify single residues that may be responsible for this phenotype. The combination of residues in C8-4 and C8-22 may lead to an altered positioning of one of the P680 chlorophylls, which causes the phenotype observed.

Mutational Effects on the OEC. While calcium and chloride are known to be essential cofactors in the process of oxygen evolution in PS II, their role in water-splitting chemistry remains largely unknown (reviewed in ref *36*). Several PS II mutants lacking extrinsic lumenal proteins or with mutations in lumenal regions of the chlorophyll binding proteins CP43 and CP47 have been unable to grow under conditions of calcium and/or chloride depletion. Mutants most sensitive to calcium depletion are those lacking the extrinsic protein PsbO (the "33 kDa" manganese stabilizing protein) (*37*). Mutations in CP43 and CP47 have been shown to lead to increased calcium and/or chloride requirements without an apparent destabilization of the binding of the extrinsic proteins (*26*, *38*, *39*). Since in most combinatorial mutants analyzed here the Cl^- requirement is increased much more than the Ca^{2+} requirement, the results found here are unlikely to be due to the loss of an extrinsic subunit.

This is the first time that mutations in a core reaction center protein have been shown to alter the calcium and/or chloride requirement of the OEC. The OEC is generally placed toward the D1 side of the D1/D2 core heterodimer, tacitly implying that D2 is not intimately involved in the water-splitting chemistry. The cofactors bound to D2 are not directly involved in electron-transfer processes between the OEC and P680. However, the fact that alteration of the CD loop in D2 affects ion requirements of the OEC argues for an intimate structural connection between this region and the OEC, so that structural changes on the lumenal side of D2 affect the Cl^- affinity.

One of the residues that may be closely involved in determining Cl^- affinity is His189 since mutating this residue alone has a significant impact on the chloride requirement of the OEC. This may suggest that Y_D properties affect the structure of the OEC. However, other mutants with a normal Y_D^{ox} spectrum (Figure 3) showed a major change on Cl^- dependence (Table 5), suggesting that structural changes in this region of D2 other than those mediated via Y_D are also important for determining the Cl^- affinity of the OEC.

The data on the Trp191 restoration mutants presented in Tables 4 and 5 indicate that Trp191 does not significantly affect the chloride requirement of the combinatorial mutants.

C8-4W191 showed only minor improvement over its counterpart, C8-4, in terms of photoautotrophic growth at limiting chloride concentrations, whereas in the case of C8-22 a restored Trp191 did not make a difference in the Cl^--limited photoautotrophic growth. Restoration of both Trp191 and Thr192 did make a difference in ameliorating photoautotrophic growth capabilities at limiting Cl^- concentration (compare C8-7 and C8-23 with their Trp191/Thr192 counterparts in Table 5). This is not surprising in view of the Cl^- requirement of the W191L/T192A mutant that is absent from both single mutants. Therefore, residues at positions 191 and 192 together affect the Cl^- affinity of the OEC.

Results of this study have shown that combinatorial mutagenesis combined with biophysical and biochemical techniques is a powerful tool in determining functionally and structurally important residues and can provide more information than would usually can be gleaned from studying site-directed mutants.

ACKNOWLEDGMENT

We thank Dr. Russell LoBrutto for the technical help and advice provided in obtaining the EPR spectra reported here.

REFERENCES

1. Debus, R. J., Barry, B. A., Sithole, I., Babcock, G. T., and McIntosh, L. (1988) *Biochemistry 27*, 9071−9074.
2. Metz, J. G., Nixon, P. J., Rögner, M., Brudvig, G. W., and Diner, B. A. (1989) *Biochemistry 28*, 6960−6969.
3. Debus, R. J., Barry, B. A., Babcock, G. T., and McIntosh, L. (1988) *Proc. Natl. Acad. Sci. U.S.A. 85*, 427−430.
4. Vermaas, W. F. J., Rutherford, A. W., and Hansson, Ö. (1988) *Proc. Natl. Acad. Sci. U.S.A. 85*, 8477−8481.
5. Diner, B. A., and Babcock, G. T. (1996) in *Oxygenic Photosynthesis: The Light Reactions* (Ort, D. R., and Yocum, C. F., Eds.) pp 213−247, Kluwer Academic Publishers, Dordrecht, The Netherlands.
6. Tang, X.-S., Chisholm, D. A., Dismukes, G. C., Brudvig, G. W., and Diner, B. A. (1993) *Biochemistry 32*, 13742−13748.
7. Tommos, C., Davidsson, L., Svensson, B., Madsen, C., Vermaas, W., and Styring, S. (1993) *Biochemistry 32*, 5436−5441.
8. Hays, A.-M. A., Vassiliev, I. R., Golbeck, J. H., and Debus, R. J. (1998) *Biochemistry 37*, 11352−11365.
9. Kim, S., Liang, J., and Barry, B. A. (1997) *Proc. Natl. Acad. Sci. U.S.A. 94*, 14406−14411.
10. Campbell, K. A., Peloquin, J. M., Diner, B. A., Tang, X.-S., Chisholm, D. A., and Britt, R. D. (1997) *J. Am. Chem. Soc. 119*, 4787−4788.
11. Styring, S., and Rutherford, A. W. (1987) *Biochemistry 26*, 2401−2405.
12. Rova, M., Mamedov, F., Magnuson, A., Fredriksson, P.-O., and Styring, S. (1998) *Biochemistry 37*, 11039−11045.
13. Magnuson, A., Rova, M., Mamedov, F., Fredriksson, P.-O., and Styring, S. (1999) *Biochim. Biophys. Acta 1411*, 180−191.
14. Xiong, J., Subramaniam, S., and Govindjee (1998) *Photosynth. Res. 56*, 229−254.
15. Svensson, B., Etchebest, C., Tuffery, P., van Kan, P., Smith, J., and Styring, S. (1996) *Biochemistry 35*, 14486−14502.
16. Keilty, A. T., Ermakova-Gerdes, S. Y., and Vermaas, W. F. J. (2000) *J. Bacteriol. 182*, 2453−2460.
17. Tommos, C., Madsen, C., Styring, S., and Vermaas, W. (1994) *Biochemistry 33*, 11805−11813.
18. Manna, P., LoBrutto, R., Eijckelhoff, C., Dekker, J., and Vermaas, W. (1998) *Eur. J. Biochem. 251*, 142−154.
19. Durrant, J. R., Klug, D. R., Kwa, S. L. S., van Grondelle, R., Porter, G., and Dekker, J. P. (1995) *Proc. Natl. Acad. Sci. U.S.A. 92*, 4798−4802.
20. Peterman, E. J. G., van Amerongen, H., van Grondelle, R., and Dekker, J. P. (1998) *Proc. Natl. Acad. Sci. U.S.A. 95*, 6128−6133.
21. Vavilin, D. V., and Vermaas, W. F. J. (2000) *Biochemistry 39*, 14831−14838.
22. Vermaas, W., Charité, J., and Eggers, B. (1990) in *Current Research in Photosynthesis* (Baltscheffsky, M., Ed.) Vol. 1, pp 231−238, Kluwer Academic Publishers, Dordrecht, The Netherlands.
23. Shen, G., Boussiba, S., and Vermaas, W. F. J. (1993) *Plant Cell 5*, 1853−1863.
24. Ermakova-Gerdes, S., Shestakov, S., and Vermaas, W. (1995) in *Photosynthesis: from Light to Biosphere* (Mathis, P., Ed.) Vol. I, pp 483−486, Kluwer Academic Publishers, Dordrecht, The Netherlands.
25. Rippka, R., Deruelles, J., Waterbury, J. B., Herdman, M., and Stanier, R. Y. (1979) *J. Gen. Microbiol. 111*, 1−61.
26. Tichy, M., and Vermaas, W. (1998) *Biochemistry 37*, 1523−1531.
27. Bittersmann, E., and Vermaas, W. (1991) *Biochim. Biophys. Acta 1098*, 105−116.
28. Lince, M. T., and Vermaas, W. (1998) *Eur. J. Biochem. 256*, 595−602.
29. Chu, H.-A., Nguyen, A. P., and Debus, R. J. (1994) *Biochemistry 33*, 6137−6149.
30. Chu, H.-A., Nguyen, A. P., and Debus, R. J. (1995) *Biochemistry 34*, 5839−5858.
31. Lin, X., Murchison, H. A., Nagarajan, V., Parson, W. W., Allen, J. P., and Williams, J. C. (1994) *Proc. Natl. Acad. Sci. U.S.A. 91*, 10265−10269.
32. Mulkidjanian, A. Y. (1999) *Biochim. Biophys. Acta 1410*, 1−6.
33. Deisenhofer, J., and Michel, H. (1989) *EMBO J. 8*, 2149−2169.
34. Ponamarev, M. V., Schlarb, B. G., Howe, C. J., Carrell, C. J., Smith, J. L., Bendall, S. D., and Cramer, W. A. (2000) *Biochemistry 39*, 5971−5976.
35. Schatz, G. H., Brock, H., and Holzwarth, A. R. (1987) *Biophys. J. 54*, 397−405.
36. Britt, R. D. (1996) in *Oxygenic Photosynthesis: The Light Reactions* (Ort, D. R., and Yocum, C. F., Eds.) pp 137−164, Kluwer Academic Publishers, Dordrecht, The Netherlands.
37. Philbrick, J. B., Diner, B. A., and Zilinskas, B. A. (1991) *J. Biol. Chem. 266*, 13370−13376.
38. Putnam-Evans, C., and Bricker, T. M. (1997) *Plant Mol. Biol. 34*, 455−463.
39. Clarke, S. M., and Eaton-Rye, J. J. (1999) *Biochemistry 38*, 2707−2715.

BI002772D